ISSN: 2277-3754
International Journal of Engineering and Innovative Technology (IJEIT)
Volume 1, Issue 3, March 2012

Numerical Study of Turbulent Flow and Heat Transfer in Square Convergent Channel with 90° Inline Rib Turbulators

Siva Kumar. K, Dr. E. Natarajan, Dr. N. Kulasekharan

Abstract*— In this present work, the local heat transfer and Nusselt number of developed turbulent flow in convergent/divergent square duct have been investigated computationally. Experimental results for this configuration are reported elsewhere [14] in three different channels viz., smooth square duct, ribbed convergent square duct and ribbed divergent square duct. The angle of convergence of the duct is about 1˚. Among the three channel shapes, the convergent square duct with ribs alone is considered for carrying out the present computational analysis. The computational analysis was conducted within the range of Reynolds number from 10,000 to 77,000. The heat transfer performance of the convergent ducts from the present analysis is compared with that of the experimental data reported and good agreement has been found. Because of the stream-wise flow acceleration, the local heat transfer characteristics of the convergent ducts are quite different from those of the straight duct. There is no trend of flow and heat transfer development or flow becoming fully developed in the case of convergent ducts.

***Index Terms*— Rib Turbulators, Aspect Ratio, Heat Transfer, Rib Spacing.**

I. INTRODUCTION

In internal cooling of gas turbine blades, coolant air is circulated through serpentine passages and discharged through the bleed holes along the trailing edge of the blade (Fig.1). With rotation, the flow is subjected to Coriolis a force which induces secondary flow in planes perpendicular to the stream wise flow direction. This results in the migration of core fluid towards the trailing wall for radially-outward flow. Thus, while rotation destabilizes the flow and enhances heat transfer along the trailing wall, they stabilize the flow and reduce the heat transfer along the opposite wall. In addition, centrifugal buoyancy influences the radially- outward flow along the heated walls and at high rotation numbers, can have a significant effect on the surface heat transfer.

Turbulent heat transfer and fluid flow characteristics of air in rib-roughened tubes, annuli, ducts and between parallel plates have been studied extensively because of their important applications. Such a heat transfer enhancement method is widely used in cooling passages of gas turbine blade, compact heat exchangers, fuel elements in advanced gas-cooled reactor electronic cooling devices, etc. Taking the cooling passages is usually approximated by a rectangular duct with a pair of opposite rib-roughened walls. In the computational investigations reported in the literature, the internal cooling passages of a gas turbine have been modelled by either square or rectangular channels having two ways.

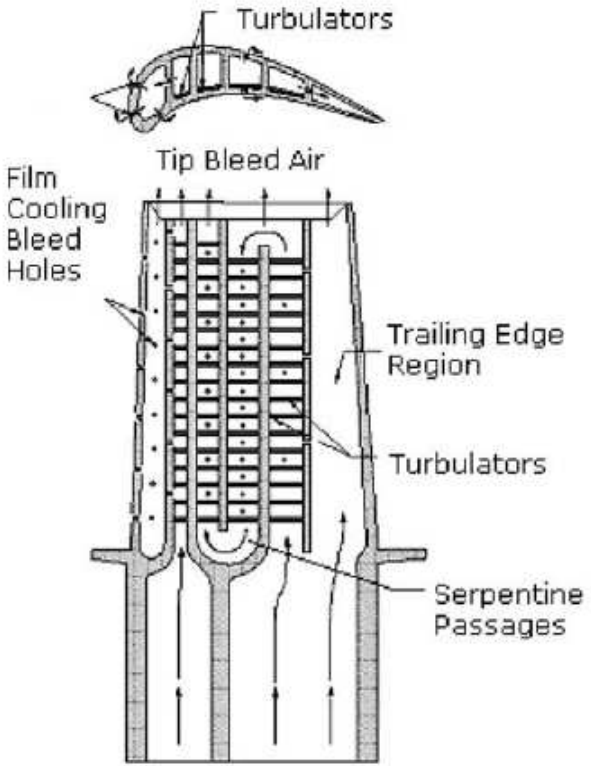

Fig. 1. Schematic sketch of a typical gas turbine blade.

As presented by Abuaf and Kercher (1), in typical airfoils with multipass cooling circuits, the cross-sectional area of radial passage usually varies along the passage from root to tip. In other words, the cooling passages are actually convergent to some extent. Such a geometric variation may induce substantial difference in both flow and heat transfer characteristics compared to those models with straight rectangular channel. However, no significant study has been found in the existing literature that deals with heat transfer in ribbed roughened convergent ducts. Wang et al (2001) found that for a smooth square duct a mild stream wise variation of cross sectional area may induce significant difference in the local and average heat transfer behaviors.

A large number of experimental studies are reported in the literature on internal cooling in turbine blade passages, particularly for square coolant passages [2-7]. In a recent study, heat transfer in a rectangular channel with aspect ratio AR = 4:1 has been reported by Zhou et al. [8] for smooth surfaces and by Griffith et al. [9] for rib-roughened surfaces. Non-monotonic behavior with respect to the rotation number was observed for the smooth channel [8], while for the ribbed channel, the trailing surface heat transfer showed

ISSN: 2277-3754
International Journal of Engineering and Innovative Technology (IJEIT)
Volume 1, Issue 3, March 2012

strong dependence on the rotation number [9]. Data for 1:4 AR duct with rotation is limited, with Agarwal et al. [10] recently reporting mass transfer data for smooth and ribbed ducts with rotation.

Most of the earlier computational studies on internal cooling passage of the blades have been restricted to three-dimensional steady RANS simulations [11-13]. The flow and heat transfer through a two pass smooth and 45˚ rib roughened rectangular duct with an aspect ratio of 2 has been reported by Al-Qahtani et al [14,15] using Reynolds stress turbulence model. They have found reasonable agreement with experimental studies however, in certain regions there were some significant discrepancies.

In this study, computational validation is conducted to find the developing heat transfer and friction characteristics of turbulent flow in ribbed convergent ducts with uniform heat flux boundary condition. Thermal performance comparison among convergent ducts has been conducted under three conditions.

II. Experimental Setup

A schematic of the experimental system as reported in [14] is shown in Fig.2. This is an open test loop, with the room air being drawn by a 3.5 KW blower situated at the downstream end of the test loop. The forced air goes through an entrance section pre-plenum, test section an after plenum and a 60 mm diameter, 1440 mm length pipe, equipped with a multiport averaging Pitot tube to measure the flow rate.

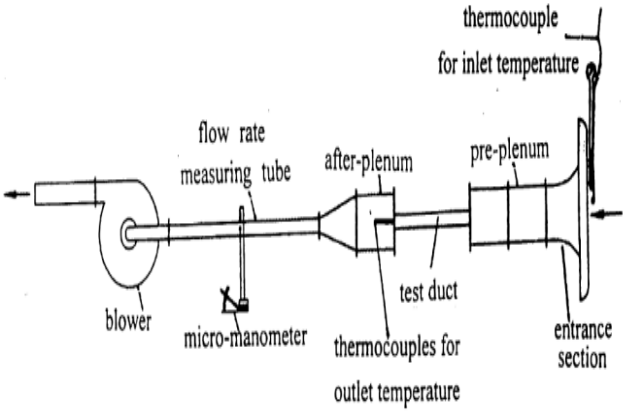

Fig.2. Schematic diagram of test apparatus by [14].

The ribs are manufactured as integral parts on two opposite walls of the duct. The convergent square ribbed duct has largest cross-section of 58 x 58 mm2 and a smallest cross-section of 41 x 41 mm2. Each test duct is 500 mm long. The rib size and arrangement are shown in Fig.3. The value of e/Dm = 0.081 and P/E = 17.8, where Dm is the duct average value of hydraulic diameter. To get a detailed distribution of the local heat transfer coefficient, 120 thermocouples are imbedded in one of the ribbed walls along its centre line for measurement.

III. Nomenclature

A	surface area. m^2
D_h	hydraulic diameter
D_m	average hydraulic diameter, m
e	rib height. m
f	friction factor
h	heat transfer coefficient, W/m^2K
k	thermal conductivity, W/m K
L	axial length of duct, m
m	mass flow rate, kg/s
Nu	Nusselt number
Nu_s	Nusselt number of smooth side
Nu_r	Nusselt number of ribbed side
Nu_t	duct average Nusselt number
Δp	pressure drop of duct, pa
Q	heat transfer rated, W
Re	Reynolds number
Re_m	Reynolds number based on D_m
T	temperature, K
T_w	wall temperature, K
x	stream wise direction

IV. Data Reduction

The local heat transfer coefficient has been calculated from the total net heat transfer rate and the difference between the local wall temperature and the local bulk mean air temperature.

$$h_x = \frac{(Q - Q_{loss})}{A(T_{w,x} - T_{b.x})} \text{--------(1)}$$

The local wall temperature used in Eq. (1) was read from the output of the thermocouple. The local bulk air temperature of air is calculated by using the following equation:

$$T_{b,x} = T_{in} + \frac{(Q - Q_{loss})A(x)}{Amc_p} \text{---(2)}$$

Where A (x) is the heat transfer surface area from the duct inlet to the position where the local heat transfer coefficient was determined.

$$Nu_x = \frac{h_x D_m}{k} \text{----------(3)}$$

$$Nu = \frac{(Q - Q_{loss})/D_m}{Ak(T_w - T_m)} \text{------(4)}$$

The characteristic length, the reference temperature and the average wall temperature have been determined by.

$$D_m = \frac{D_{h.in} - D_{h.out}}{2} \text{--------(5)}$$

$$T_m = \frac{T_{b,in} + T_{b,out}}{2} \text{--------(6)}$$

$$T_w = \frac{1}{A}\int_0^A T_{w.x} dA \text{----------(7)}$$

$$\mathrm{Re}_m = \frac{U_m D_m}{2} \text{--------------(8)}$$

Where Um is the duct mean cross-sectional average velocity. This is equal to the cross-section average velocity at the duct mid section.

ISSN: 2277-3754
International Journal of Engineering and Innovative Technology (IJEIT)
Volume 1, Issue 3, March 2012

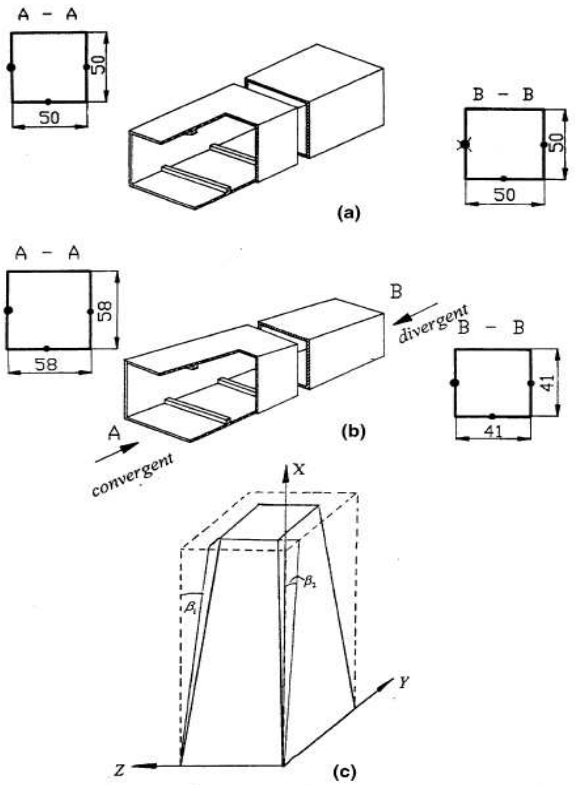

Fig.3. Diagram of test tube: (a) ribbed duct of constant cross section; (b) ribbed divergent/ convergent duct; (c) schematic diagram showing the inclination angle [14].

V. NUMERICAL SOLUTION PROCEDURE

The computational model studied in the present study includes a segment of the inlet plenum and the test section. Inlet for the computational domain is the inlet to the domain, so that more realistic flow with entry effect can be simulated for the test section. The flow is assumed to leave the test section to ambient with a zero static pressure boundary condition at the outlet.

In this study, a commercial CFD program Fluent 6.3 has been used to carry out the numerical study. Fluent 6.3 includes several turbulence models. Computations are performed for laminar and turbulent flows depending on the Reynolds number. The energy equation is solved neglecting radiation effects. The renormalization-group RNG k−ε model is employed as the turbulence model for turbulent flow. The Reynolds averaged Navier–Stokes equations are solved numerically in conjunction with transport equations for turbulent kinetic energy and dissipation rate. Full buoyancy effects are included in transport equations. Near wall regions are fully resolved for y+ values between 0.1 and 0.5.

In the present study, structured computational cells were created with a fine mesh near the plate walls and coarse mesh away from the plate walls with the help of bi-exponent ratio scheme in GAMBIT 2.4. Steady inline solver was used with second order up winding scheme for convective terms in the mass, momentum, energy, and turbulence equations for both laminar and turbulent flows. For pressure discretization the PRESTO scheme has been employed while for pressure–velocity coupling discretization the SIMPLE-algorithm has been used.

The general forms of the governing equations for this problem are:

$$\frac{\partial \rho u_j}{\partial x_j} = 0 \text{ ----------(9)}$$

$$\frac{\partial}{\partial x_j}(\rho u_j u_i) = \frac{\partial \rho}{\partial x_j} + \frac{\partial}{\partial x_j}(\tau_{ij} - \overline{\rho u' u'_j}) \text{ --(10)}$$

$$\frac{\partial}{\partial x_i}[u_i(\rho E + p)] = \frac{\partial}{\partial x_j}\left[(\lambda + \frac{C_p \mu_t}{\Pr_t})\frac{\partial T}{\partial x_j} + u_i(t_{ij})_{eff}\right] \text{ ---(11)}$$

$$-\overline{\rho u' u'_j} = 2\mu_t - \frac{2}{3}\rho k \partial_{ij} \text{ -------(12)}$$

Continuity, momentum and energy equations are solved by the finite volume method with structured meshes and the coupling between the velocity and pressure given by the SIMPLE algorithm. The advection terms in the momentum, energy, mass transport, turbulent kinetic energy and specific dissipation equations were discretized using the second order upwind algorithm. Grid independence studies resulted in meshes having about 1, 50,000 elements for each case.

The convergence criteria were 10-4 for velocity, 10-6 for k and u and 10-8 for energy. The inlet boundary conditions were set as velocity inlet and mass flow rate with the outlet conditions set as pressure. The heat flux boundary condition was used in all the surfaces with no-slip.

VI. RESULT AND DISCUSSION

A. 90˚ Rib Bed Plate

The local Nu for the 90˚ rib plate shown in Fig.4 illustrates that the local Nu first increases before the first rib due to the entrance effect. The Nu increases as the boundary layer thickness increases along the plate. Again it increases after the first rib especially for a short distance because the boundary layer is disrupted by the rib.

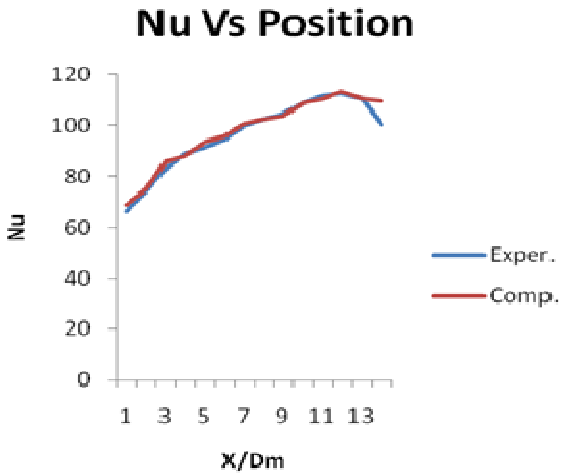

Fig.4. Local Nu for the 90˚ rib bed plate.

ISSN: 2277-3754
International Journal of Engineering and Innovative Technology (IJEIT)
Volume 1, Issue 3, March 2012

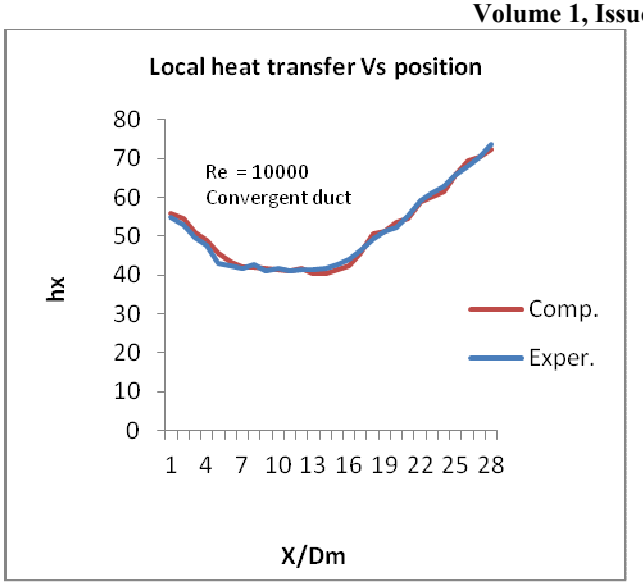

Fig.5. Local Nu for the 90˚ rib bed plate.

The local heat transfer for the 90˚ rib attached plate shown in Fig.5 illustrates that the local heat transfer first decreases before the first rib due to the entrance effect. Then the local heat transfer increases as the boundary layer thickness increases along the plate. It then increases after the first rib especially for a short distance, because the boundary layer is disrupted by the rib.

This phenomenon is illustrated in Figs. 6 and 7, by the distinct vortex after the first rib, which enhances the turbulence mixing of the flow field, to increase the heat transfer. Although the thermal boundary layer was disrupted, the velocity in the region near the surface between the two ribs is lower and so the overall trend for the Nu decreases along the plate. The local Nu increases at the test channel outlet, because the fluid flow is not constrained after the last rib. The velocity near the surface is increased, resulting in enhancement of the heat transfer. This phenomenon can also be found Fig.7, where the vortex after the second rib is smaller than the first one.

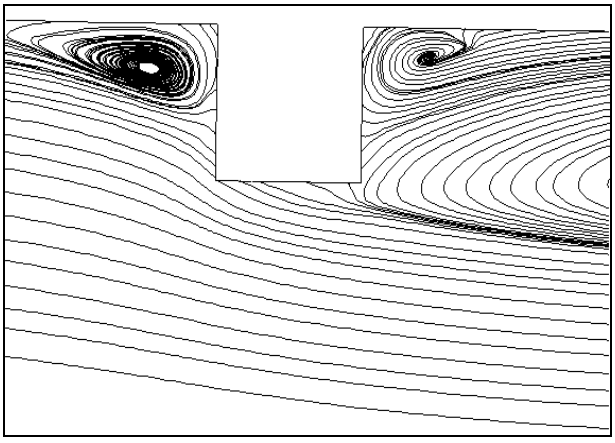

Fig. 6 Flow fields on the center cross section for the first -90˚ rib bed plate.

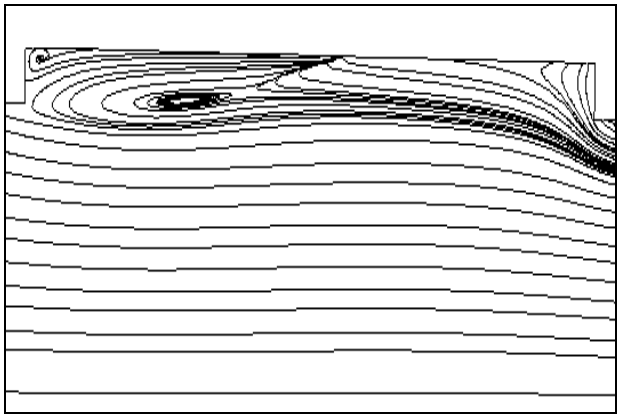

Fig.7. Flow fields in between two rib.

B. Numerical Simulations for 90˚ Ribs

The design includes continuous 90˚ ribs arranged as shown in Fig. 8. The channel is of convergent square ribbed duct with largest cross-section of 58 x 58 mm2 and the smallest cross-section of 41 x 41 mm2 and test duct has 500 mm long. Grid independence studies resulted in meshes having about 150000 elements for each case. The plane where the temperature and pressure measured on from the duct is shown in Fig.8.

C. Velocity and Temperature

The velocity a contour of a square 90˚ rib on chosen planes is shown in Fig. 9 and discussed in this section. A vertical and a horizontal plane passing through the mid of the channel are considered. Figure 9 shows the contours of velocity magnitude on these planes. Along these planes it can be observed that the velocity at inlet is lower than at the outlet of the duct, due to the flow acceleration in the stream-wise direction. The naturally expected acceleration in a converged channel flow is further augmented by the flow blockage offered by the ribs on the opposing walls, which is evident from the contours on the mid vertical plane.

Fig.10. shows the central core flow of air which gets deflected away from the top and bottom wall surfaces. This flow deflection is due to the eddy formation from ribs; contours show the stream-wise velocity on the vertical plane. The contours of temperature for the square convergent duct on the mid horizontal plane and vertical planes are shown in Figs. 11 and 12. Near the ribs the temperatures are higher than the core of the duct, because the cold air entering the channel inlet is less.

Fig. 13 shows the temperature distribution contours on the left side wall, bottom wall and along the rib surfaces. Side wall and rib surface temperature contours show the pattern of flow evolution or eddy formation from the ribs. Bottom wall surface temperature contours show the impingement action of eddies from the rib. View from the duct outlet side shows regions of high temperatures, which might be due to the interaction of boundary conditions on the side, ribs and bottom wall surfaces. Another reason could be the recirculation zone forming in the corner, which reduces the effective heat transfer from the corners.

ISSN: 2277-3754
International Journal of Engineering and Innovative Technology (IJEIT)
Volume 1, Issue 3, March 2012

The contours of heat transfer coefficient on the side wall, bottom wall and rib surfaces are shown in Fig.14. The effect of plenum flow entering the test section can be observed from the peak value of local heat transfer coefficient 'h' on the side and bottom walls. The edges of the ribs show higher heat transfer coefficient values due to the edge effect and the flow separation from the rib front corners. View from the exit side of the test section shows the rib rear side 'h' values which are lower than that in the rib front side.

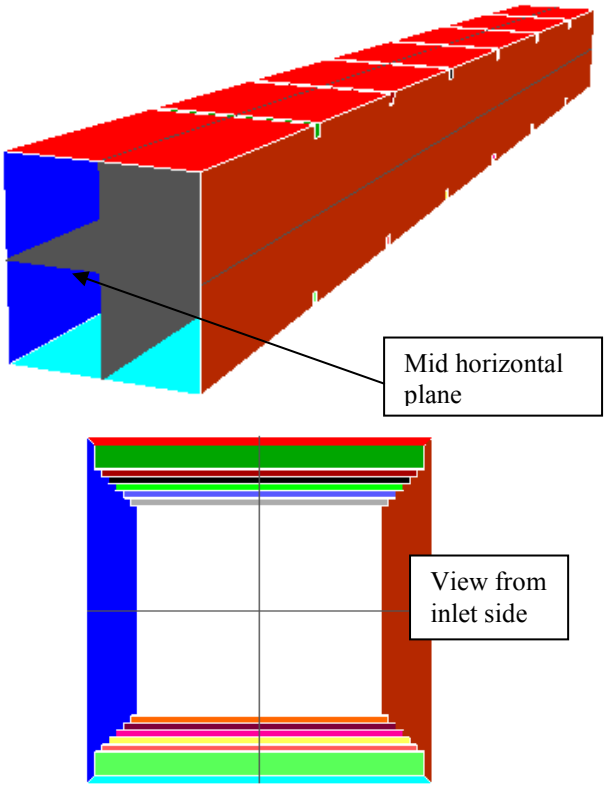

Fig.8. Planes used for data extraction

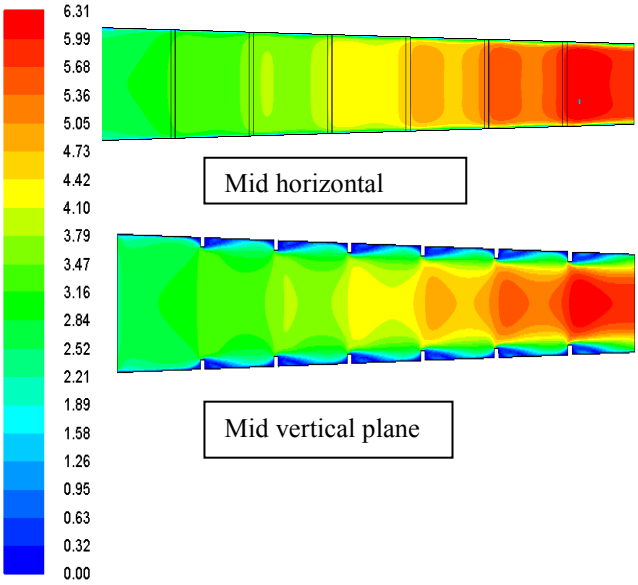

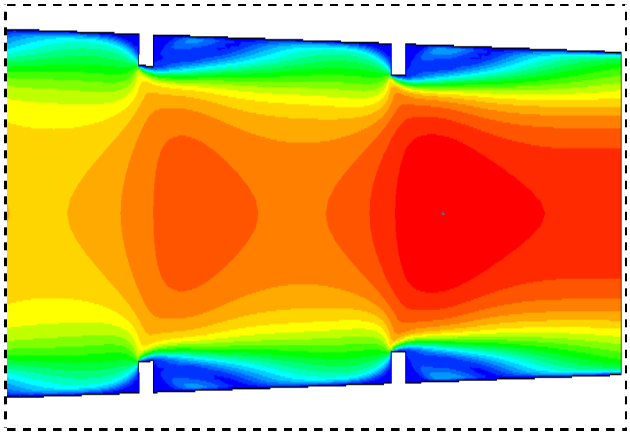

Fig.9. Contours of velocity magnitude on a vertical plane

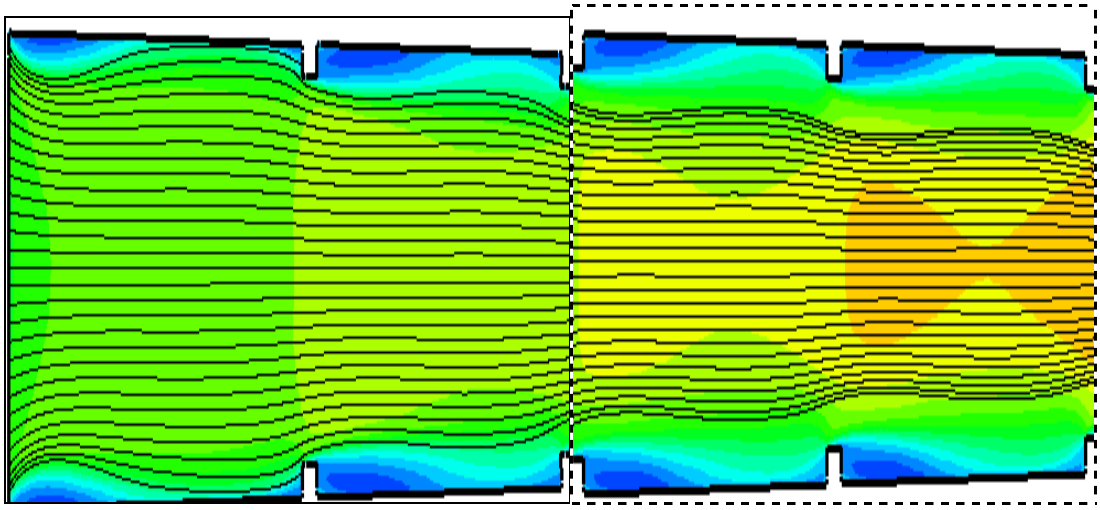

Fig.10.Central core flow – deflected away from the wall due to eddy formation from ribs; contours show the stream-wise velocity on the vertical plane

ISSN: 2277-3754
International Journal of Engineering and Innovative Technology (IJEIT)
Volume 1, Issue 3, March 2012

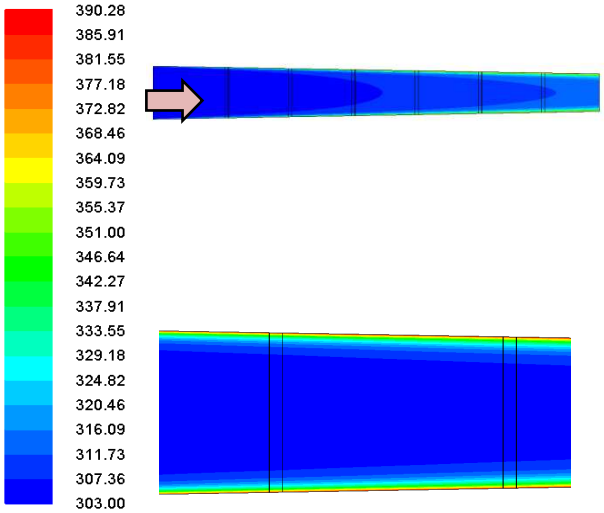

Fig.11. Contours of temperature on middle horizontal plane

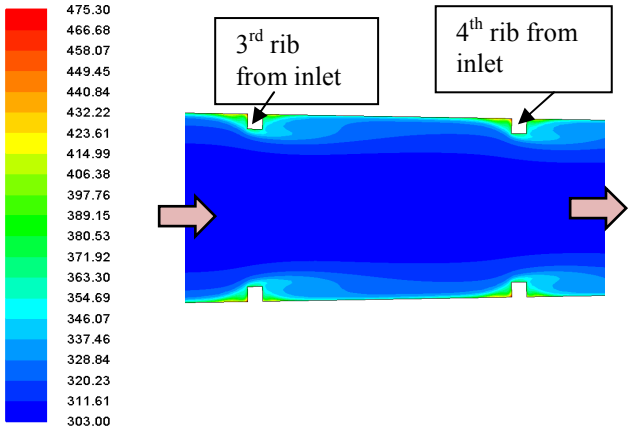

Fig.12. Contours of temperature on a vertical plane

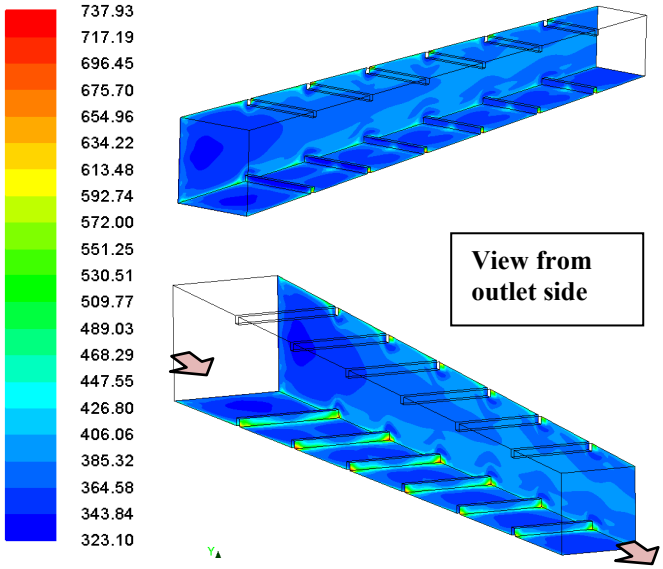

Fig.13. Contours of temperature (K) on the side and bottom wall

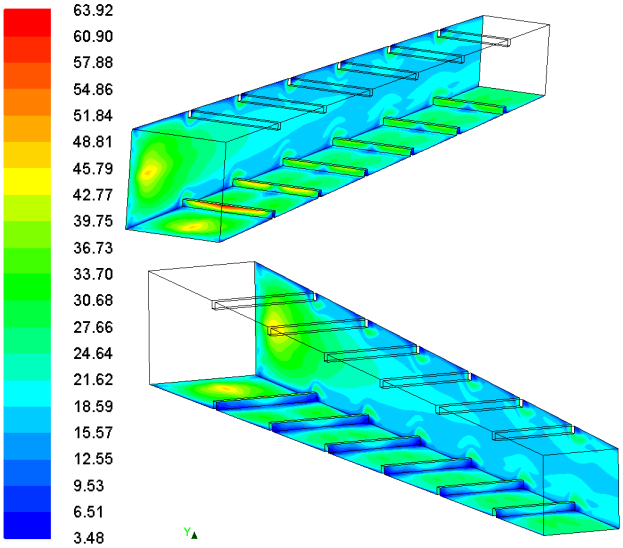

Fig. 14.Contours of heat transfer coefficient 'h' (W/m^2-k) on the side and bottom wall

VII. CONCLUSION

The work reported here is a computational analysis of the convergent square duct with 90° ribbed inline arrangement. Comparison of the Nusselt number between experiment and CFD simulations and also different types of contours (velocity, temperature and heat transfer coefficient) are presented.

REFERENCES

[1] N.Abuaf, D.M. Kercher., heat transfer and turbulence in a turbine blade cooling circuit. ASME J. turbo machinery 116, 169-177.

[2] J.C. Han, J.S.Park, Developing heat transfer in rectangular channel with rib turbulators, Int.J. Heat Mass Transfer 31 (I) (1988) 183-195.

[3] J.C.Han, Heat transfer and friction characteristics in rectangular channels with rib turbulators, J. Heat Trasnfer 110 (1988) 321-328.

[4] J.H.Wagner, B.V. Johnson, R.A. Graziani. F.C. Yeh, Heat transfer in rotation serpectine passages with trips normal to the flow, J. Turbo mach. 114 (1992) 847-857.

[5] B.V.Johnson, J.H.Wagner, G.D. Steduber, F.C.Yeh, Heat transfer in rotating serpentine passages with trips skewed to the flow, J.Turbomach. 116 (1994) 113-123.

[6] B.V. Johnson, J.H. Wagner, G.D Steuber, effect of rotation on coolant passage heat transfer, NASA contractor Report – 4396, vol. II, 1993.

[7] Y.Chen, D.E Nikitopoulos, R.Hibbs, S.Acharya, T.A. Myrum, Detailed mass transfer distribution in a ribbed coolant passage, Int. J. Heat mass transfer 43 (200) 1479-1492.

[8] T.S.Griffith. L.Al-Hadhrami. J.C. Han, Heat transfer in rotating rectangular cooling channels with angled ribs, J. Heat Transfer 124 (2002) 617-625.

[9] P.Agarwal, S. Acharya, D.E. Nikitopoulos, Heat transfer I 1:4 rectangular passages with rotation, J. Turbo mach 125 (2003) 726-733.

ISSN: 2277-3754
International Journal of Engineering and Innovative Technology (IJEIT)
Volume 1, Issue 3, March 2012

[10] D.L. Rigby, E.Steinthorsson, A.A. Ameri, Numerical prediction of heat transfer in a channel with ribs and bleed, ASME Paper 97- GT-431, 1997.

[11] T.Bo. H.Lacovides, B.E. Launder, Developing buoyancy modified turbulent flow in ducts rotating in orthogonal mode, J. Turbomach.117 (1995) 474-484.

[12] H.Lacovides, Computation of flow and heat transfer through rotating ribbed passage, Int. J. Heat Fluid flow, 19 (1988) 393-400.

[13] M.Al.Qantani, H.C. Chen, J.C. Han, A numerical study of flow and heat transfer in rotating rectangular channels (AR = 4) with 45˚ rib turbulators by Reynolds stress turbulence model. J. Heat Transfer 125 (1) (2003) 19-26.

[14] L.H.Wang, W.Q.Tao, Q.W.Wang, T.T.Wong., Experimental study of developing turbulent flow and heat transfer in ribbed convergent/divergent square duct. Int.J. of Heat and fluid flow 22 (2001) 603-613.

AUTHORS PROFILE

Mr. Sivakumar Karthikeyan is currently working as an Assistant Professor in the Department of Mechanical Engineering at Valliammai Engineering college. He did his masters degree in Thermal Engineering at National Institute of Technology, Trichy, India and bachelor's degree in Mechanical Engineering at Adhiparasakthi Engineering college, Melmuruvathur, India. He has more than14 years of teaching and 3 years of research experience. He is life member of ISTE. He has presented 7 national/international conferences so far. He has also served as a reviewer for Heat and Mass Transfer Journal.

Dr. E. Natarajan was born on 13th February 1967 in Tamil Nadu State of India. He obtained his degree in Bachelor of Engineering with the specialization of Mechanical Engineering from Madras University in 1984. He secured University first rank in B.E., for which he was also awarded the Sir Gabriel Stokes Prize (Mechanical Branch) 1988 and Dr.A.L.Mudaliar Prize 1988. He obtained his M.Tech degree in Mechanical Engineering from IIT Madras Chennai in 1990. He obtained his Ph.D in the area of Fluidized Bed Biomass Gasification from Anna University in 1999. He has more than 22 years of teaching and research experience an currently serving as Professor in Institute for Energy Studies in the Mechanical Engineering Department of Anna University,Chennai, India .

Dr. Kulasekharan Narasingamurthi is currently Technical Lead in GE Appliances at India. His current roles includes performing conjugate flow and thermal studies in Home appliances using commercial computational fluid dynamic tools. He supports NPI and existing product development/improvement activities. Previous to this role, he was with Caterpillar India performing analysis for automotive systems and components. He did his doctoral research work in Mechanical Engineering at Indian Institute of Technology Madras, Chennai, India. He worked with Prof. BVSSS Prasad of Mechanical Engineering. His research area was conjugate heat transfer studies in gas turbine first .stage guide vane using CFD.He did his masters degree in Thermal Engineering at National Institute of Technology, Trichy, India and bachelors degree in Mechanical Engineering at Institute of Road and Transport Technology, Erode, India. He is life member of ISHMT, Annual member of ASME. He has published his works in 2 international journals and 10 national/international conferences so far. He has also served as a reviewer for ASME Turbo Expo international conferences twice. In addition, he also has 4 years of experience lecturing to under graduate and post graduate engineering students in India.